Scientia Iranica A (2015) 22(1), 1–14

Sharif University of Technology
Scientia Iranica
Transactions A: Civil Engineering
www.scientiairanica.com

Local scour profiles downstream of adverse stilling basins

H. Khalili Shayan and J. Farhoudi*

Department of Irrigation and Reclamation, University of Tehran Karaj, Alborz, P.O. Box 31587-4111, Iran.

Received 3 December 2012; received in revised form 3 February 2014; accepted 29 September 2014

KEYWORDS
Scour profiles;
Time dependence;
Similarity;
Adverse stilling basin;
Submerged jet;
Sluice gate.

Abstract. In this paper, scour profiles downstream of adverse stilling basins, due to the submerged jet issuing from a sluice gate, were investigated. Experiments were conducted in a wide range of sediment sizes, incoming flow Froude numbers, tailwater depths, length and slope of the stilling basin. The results showed that the scour profiles at any bed slope are similar in shape. However, the longitude evolution of scour profiles and the volume of eroded materials increased in accordance with the slope of the basin. It was observed that the maximum depth of the scour hole occurs in the vicinity of the side walls and slightly decreases towards the centerline. A polynomial equation was derived to describe the nondimensional scour profiles at different slopes. Based on experimental data, the scour characteristics have been correlated with the time of equilibrium stage by developing some empirical relationships. Finally, a power-law equation was derived and fully defined to include the dimensions of the scour hole time scale and the geometry of the sluice gate.

1. Introduction

Scour phenomena in the vicinity of hydraulic structures are considered an important problem, as they challenge its stability. Hydraulic jump at the downstream of a stilling basin contains large velocities, which cause high local shear stresses that generally exceed the critical shear stresses for the incipient motion of bed materials. If the depth of the scour hole is large enough, the stability of the upstream stilling basins may be endangered. A way to prevent this occurring is to design the foundation of a stilling basin in a safe location. The prediction of maximum local scour depth at the downstream of hydraulic structures is considered a classical problem in river engineering. The scour phenomena at the downstream of grade control structures have been studied from different viewpoints. Laursen [1] firstly reported the similarity of scour profiles developed by a horizontal jet, without any theoretical implication. Breusers [2] investigated the time variation of scour holes, due to the flow over and under an estuary closure structure, without any hydraulic jump. He suggested a power-law equation to estimate the scour depth at any time. Farhoudi and Smith [3] applied the findings of Breusers [2] to determine the time scale of a scour hole downstream of a spillway apron, due to hydraulic jump. Hassan and Narayanan [4] studied the flow characteristics and the similarity of scour profiles downstream of an apron, due to a submerged jet issuing from a sluice opening. They used mean velocity distribution in a rigid model to develop a semi-empirical theory to estimate the temporal rate of scour depth. Farhoudi and Smith [5] studied the scour process downstream of hydraulic jump, featuring the characteristic parameters defining the scour hole. They demonstrated that the development of a local scour hole downstream of the apron in the passage of time shows a certain geometrical similarity, and a nondimensional scour profile can be presented by a unified equation. Chatterjee et al. [6] studied the local scour downstream of an apron due to a submerged

*. *Corresponding author. Tel./Fax: +98 263 2241119*
E-mail address: jfarhoudi@ut.ac.ir (J. Farhoudi)

jet issuing from a sluice opening, and developed an empirical equation for the time variation of scour depth to reach an asymptotic stage. Dargahi [7] presented an experimental study to examine the similarity of scour profiles and scour geometry. No experimental evidence was found in support of the similarity assumption for temporal development of the scouring process. Power-law type equations were introduced to predict scour geometry, mainly in terms of controlling scour parameters (the head above the spillway crest and the grain size of the sediment bed). Dey and Sarkar [8] carried out an experimental investigation into the effects of different parameters on scour depth due to submerged horizontal jets. The particular geometrical similarity of scour profiles at different times has been exhibited and expressed by a combination of two polynomials. Dey and Sarkar [9] investigated the effects of upward seepage on a scour hole at the downstream of an apron due to submerged jets. They reported that the maximum scour depth increases linearly with an increase in upward seepage velocity. Oliveto et al. [10] reported no similarity for scour hole profiles at the downstream of a spillway with a positive-step stilling basin. Ghodsian et al. [11] carried out an experimental study on local scour due to free fall jets in non-uniform sediments. They reported that at the equilibrium state, the median size of sediment D_{50} in the armor layer in the scour hole is about the same as D_{90} of the original sediment.

It is understood that any alterations in channel geometry, such as the adverse slope of a stilling basin, will change the characteristics of hydraulic jump, and, therefore, it influences downstream of such structures. Since the adverse aprons would increase energy loss and decrease the length of the hydraulic jump, it could be recommended as an economical replacement to classical stilling basins, as detailed by McCorquodale and Mohamed [12], and Pagliara and Peruginelli [13]. The results of these occurrences would influence the dimensions of the scour hole downstream of adverse aprons. On the other hand, the hydraulic jump on such aprons accompanies some instabilities on the hydraulic jump exiting from the basin [13-15]. This phenomenon may increase the characteristics of the scour hole, such as its depth and length. Therefore, the results of these two reciprocal effects have to be studied for achieving some novel recommendations for designers.

In this paper, the scour phenomena at the downstream of adverse stilling basins issuing from a submerged sluice gate, were investigated. The purpose of this research is to understand the effect of an adverse rigid apron on the similarity profiles. Also, experimental data were used to present some empirical equations for estimating the scour characteristics at the equilibrium stage and the time scale of the scour hole.

2. Experimentation

In order to evaluate the scour profiles downstream of a submerged sluice gate with an adverse rigid apron, some experiments were conducted in a rectangular Plexiglas-walled flume, 4.9 m long and 0.41 m width having a recirculation flow system. The schematic diagram of the experimental setup is shown in Figure 1(a). A sluice gate with gate openings (w) of 1.4, 2, and 2.5 cm, followed by a stilling basin, was installed in the flume. The 1.18 m apron was made of Plexiglas. Seven values of bed slopes ($S_o = -\tan\theta$), including -0.156, -0.0956, -0.0764, -0.0532, -0.0316, -0.0129, and 0, were used for the stilling basin, followed by an alluvial bed of 0.15 m depth and 1.8 m length constructed across the whole width of the flume. In order to have a mobile bed, three uniformly graded sands of mean diameters, $D_{50} = 1.78$, 1.11, 0.58 mm, and a density of $\rho_s = 2650$ kg/m^3 were used to fill the sediment recess section. A sand trap was placed downstream of the alluvial bed to prevent any incidental transportation of the fine sand into the flow system. Experiments in a wide range of sediment size (D_{50}), length of stilling basin ($\frac{L}{w}$) and bed slope ($S_o = -\tan\theta$), approaching Froude number ($\mathrm{Fr}_1 = \frac{q}{\sqrt{g y_1^3 \mathrm{Cos}\theta}}$) and tailwater depth ($\frac{y_t}{y_1}$), were performed ($q$ is flow intensity and y_1 is flow depth at the vena contracta after the sluice gate), as summarized in Table 1. Table 2 shows the sediment size distribution of the three sediment samples used in the experiments. The geometric standard deviation of the sand, $\sigma_g = \sqrt{\frac{d_{84.1}}{d_{15.9}}}$, approximately, were smaller than the threshold value proposed by Breusers and Raudkivi [16] for defining non-uniform grading ($\sigma_g = 1.35$). Moreover, since the uniformity coefficients, $C_u = \frac{D_{60}}{D_{10}}$, are less than 2, the sand materials can be considered uniform [17]. A planner tailgate was used for adjusting tailwater depth. The discharge was measured by a V-notch weir and the accuracy of the measured data was controlled by an electromagnetic flowmeter. The free surface profiles were measured using a point gauge with an accuracy of ± 0.1 mm. In order to avoid the undesirable erosion of sediment at the beginning of each experiment, the flume was slowly filled with water from the downstream section. Once the water level reached the desired depth, the experiment was run. On the basis of the previous studies conducted by Farhoudi and Smith [3,5], each test was carried out over a period of 24 hr. Although the equilibrium scour condition was not attained in this period, it was sufficient for most of the tests to reach a quasi equilibrium stage of scouring. However, Dey and Sarkar [8] reported that, in their experiments, the maximum scour depth reached its equilibrium value after 12 hr. The two-dimensional scour profiles were

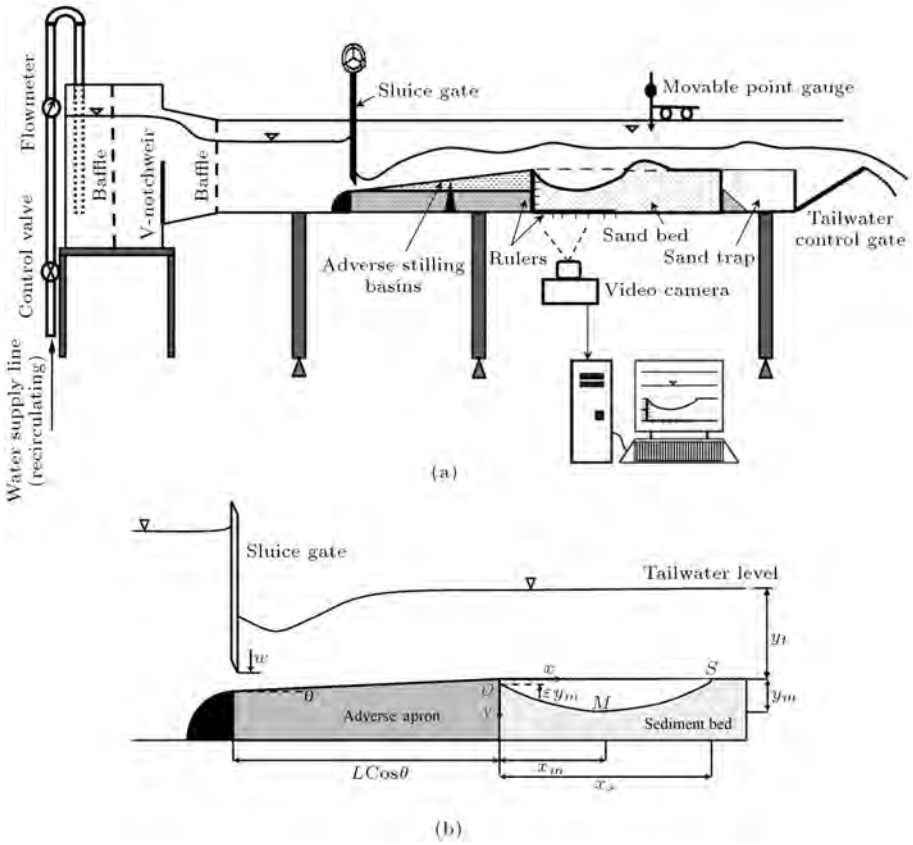

Figure 1. (a) Experimental setup. (b) Schematic sketch of the scour hole.

Table 1. Ranges of variations of different parameters in the present study.

parameter	D_{50} (mm)	$S_o = -\tan\theta$	$\frac{L}{w}$	$\frac{y_t}{y_1}$	Fr_1
Range of variations	0.58-1.78	-0.156-0	47.2-84.3	2.9-24.6	3.8-11.1

Table 2. Characteristics of sediments used in the experiments.

Name	D_{10}	$D_{15.9}$	D_{30}	D_{50}	D_{60}	$D_{84.1}$	σ_g	C_u
D_3	1.45	1.5	1.63	1.78	1.8	1.96	1.144	1.24
D_{11}	0.73	0.87	1.02	1.11	1.15	1.29	1.22	1.57
D_{141}	0.33	0.38	0.47	0.58	0.64	0.75	1.41	1.94

obtained at different times for a period of 24 hr by applying the technique of digital photography analysis. A total of 233 tests were performed and almost 3262 scour profiles were collected. Figure 2 shows the time evolution of scour holes for $S_o = -0.076$, $\mathrm{Fr}_1 = 10.76$ and $D_{50} = 1.78$ mm.

3. Results and discussion

3.1. Dimensional analysis

From dimensional analysis, the effective parameters on the scour phenomena can be expressed as (see Figure 1(b)):

$$F(\rho, v, y_t, g, q, L, \tan\theta, w, D_{50}, \rho_s, \sigma_g, C_u, \tan\phi, y_m, x_m, x_s, t) = 0, \quad (1)$$

where ρ is mass density of water, v is kinematic viscosity, ϕ is angle of repose, θ is slope angle of the adverse rigid apron, and t is the time parameter. In turbulent flows, v has a minor effect and can be neglected. Also, the effects of ρ_s, σ_g, C_u and ϕ can be overlooked, due to the uniformity of sediment grains. Considering y_m (maximum scour depth), x_m (horizontal distance of maximum scour depth from the stilling basin), x_s (length of scour hole) as dependent parameters and using the Buckingham Π theorem, result in:

$$\frac{x_m}{w}, \frac{y_m}{w}, \frac{x_s}{w} = f\left(\tan\theta, \frac{y_t}{w}, \frac{L}{w}, \mathrm{Fr}_1, \frac{t}{t_0}, \frac{D_{50}}{w}\right), \quad (2)$$

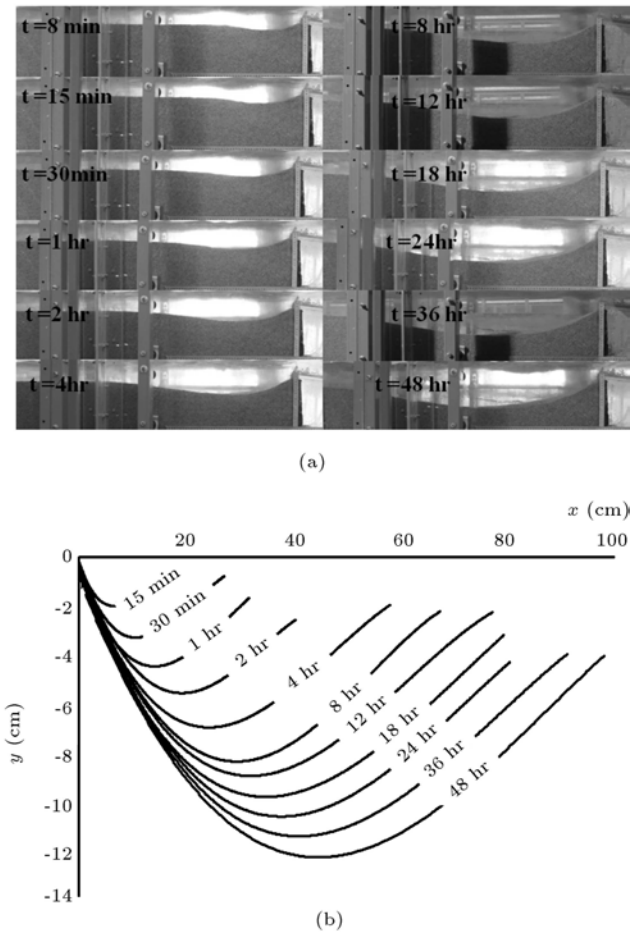

Figure 2. Scour hole profiles at different times ($S_o = -0.076, \mathrm{Fr}_1 = 9.15,\ D_{50} = 1.11$ mm).

where f is an unspecified function and $t_0 = \frac{y_t}{\sqrt{g\left(\frac{\rho_s}{\rho}-1\right)D_{50}}}$. It is assumed that the above dependent parameters are proportional to the product of the powers of the dimensionless parameters:

$$\begin{cases} \frac{x_m}{w} = \lambda_1(1+\tan\theta)^{\alpha_1}\left(\frac{y_t}{w}\right)^{\alpha_2}\left(\frac{L}{w}\right)^{\alpha_3}(\mathrm{Fr}_1)^{\alpha_4} \\ \qquad \left(\frac{t}{t_0}\right)^{\alpha_5}\left(\frac{D_{50}}{w}\right)^{\alpha_6} \\ \frac{y_m}{w} = \lambda_2(1+\tan\theta)^{\beta_1}\left(\frac{y_t}{w}\right)^{\beta_2}\left(\frac{L}{w}\right)^{\beta_3}(\mathrm{Fr}_1)^{\beta_4} \\ \qquad \left(\frac{t}{t_0}\right)^{\beta_5}\left(\frac{D_{50}}{w}\right)^{\beta_6} \\ \frac{x_s}{w} = \lambda_3(1+\tan\theta)^{\gamma_1}\left(\frac{y_t}{w}\right)^{\gamma_2}\left(\frac{L}{w}\right)^{\gamma_3}(\mathrm{Fr}_1)^{\gamma_4} \\ \qquad \left(\frac{t}{t_0}\right)^{\gamma_5}\left(\frac{D_{50}}{w}\right)^{\gamma_6} \end{cases} \quad (3)$$

in which λ_i $(i = 1,2,3)$, α_j, β_j and γ_j $(j = 1,2,3,4,5,6)$ are coefficients to be determined experimentally.

3.2. Instability of free hydraulic jump on adverse stilling basins

Establishing the adverse hydraulic jump requires overcoming the water weight upon the stilling basin. Consequently, it is required that the jump have a minimum hydrodynamic force at the supercritical section. The minimum required value of approaching Froude number depends on the length and slope of the stilling basin. An increase in length needs more hydrodynamic force for excluding the water volume on the basin. McCorquodale and Mohamed [12] concluded that it is difficult to establish this jump at Froude numbers less than 9, and required continuous tailwater adjustment to maintain a stationary position for Froude numbers less than about 4. Figure 3 shows a typical effect of

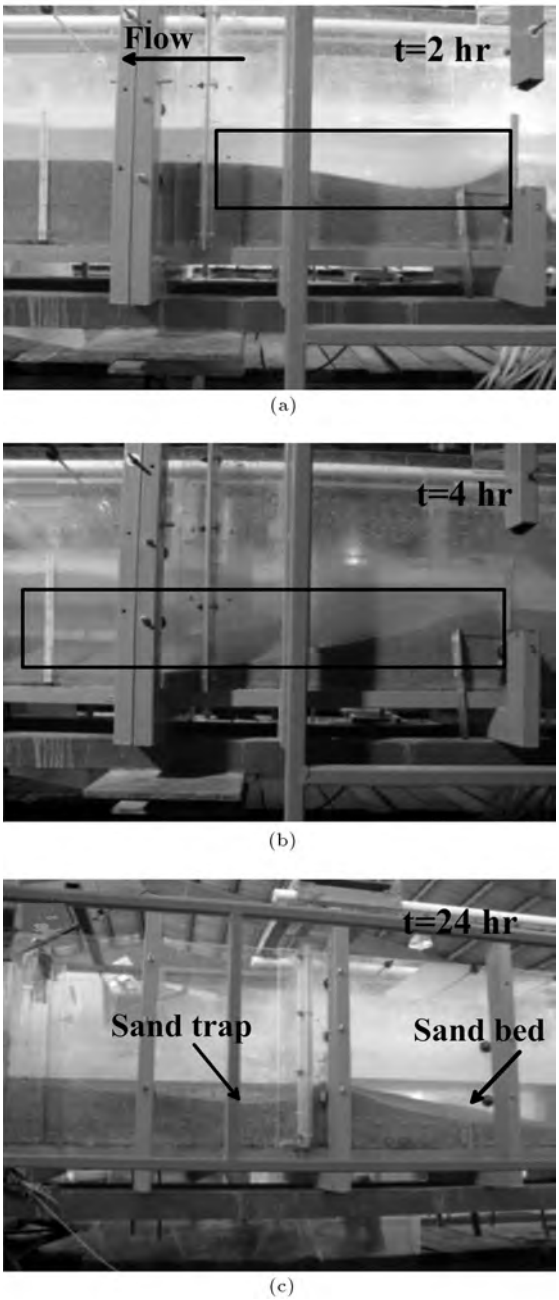

Figure 3. Time progress of scour hole at the downstream free hydraulic jump on adverse stilling basin ($S_0 = -0.053$).

unstable adverse hydraulic jump on the scour process with time. It is possible to provide a required approaching Froude number ($Fr_1 = 10.02$) and establish the hydraulic jump at the start of the test (Figure 3(a)). In spite of this, the hydraulic jump moved to the sediment bed, due to the change in tailwater depth with the scour progress, and resulted in severe erosion (Figure 3(a) and (b)). For this reason, all experiments were conducted under submerged flow conditions. It is strongly recommended that the upward stilling basins are used by an end sill or baffle blocks.

3.3. Scour profiles

Figure 2 depicts the typical time scour profiles as an example. The scour profiles vary with time, change in sediment grain size and flow conditions. In spite of this, it can be expected that a similarity exists among scour profiles at different times. This similarity implies that the scour profiles could be presented by a single curve, using appropriate variables to normalize the profiles. A temporal maximum of scour depth (y_m) was used to normalize the length and depth of the scour hole at different times (x, y). Some researchers have proposed nondimensional coordinates as $\left(\frac{x}{x_m}, \frac{y}{y_m}\right)$ and $\left(\frac{x}{x_s}, \frac{y}{y_m}\right)$ to normalize the scour profiles. Nonetheless, the dimensionless coordinate of $\left(\frac{x}{y_m}, \frac{y}{y_m}\right)$ was used in this study, due to its simplicity. The experimental values of $\frac{y}{y_m}$ against $\frac{x}{y_m}$ at different slopes of the stilling basin are plotted in Figure 4. It is shown that the scour profiles at various times are similar in nature. Attempts were made to develop an equation for the nondimensional profiles. Finally, a polynomial equation for best precision was presented as:

$$\frac{y}{y_m} = a_0 + a_1\frac{x}{y_m} + a_2\left(\frac{x}{y_m}\right)^2 + a_3\left(\frac{x}{y_m}\right)^3, \qquad (4)$$

in which a_0, a_1, a_2 and a_3 should be determined in relation to the slope of the stilling basin. By defining $K_1 = \frac{x_m}{y_m}$ and $K_2 = \frac{x_s}{y_m}$, the above coefficients are determined using the boundary conditions of the scour profile as follows (Figure 1(b)):

1. At upstream face of the scour hole, $O(0, -\varepsilon y_m)$:

$$-\varepsilon = a_0 + 0 + 0 + 0 - \varepsilon = a_0. \qquad (5)$$

2. At the maximum depth of scour hole, $M(K_1 y_m, -1)$:

$$-1 = -\varepsilon + a_1K_1 + a_2K_1^2 + a_3K_1^3 \rightarrow a_1K_1 + a_2K_1^2 + a_3K_1^3 = \varepsilon - 1, \qquad (6)$$

and:

3. $\frac{dy}{dx}(x = x_m) = 0$:

$$\frac{dy}{dx} = a_1 + 2a_2\frac{x}{y_m} + 3a_3\left(\frac{x}{y_m}\right)^2 \rightarrow 0$$
$$= a_1 + 2a_2K_1 + 3a_3K_1^2 \rightarrow a_1$$
$$= -2a_2K_1 - 3a_3K_1^2. \qquad (7)$$

4. At the downstream face of the scour hole, $S(K_2 y_m, 0)$:

$$0 = -\varepsilon + a_1K_2 + a_2K_2^2 + a_3K_2^3 \rightarrow a_1K_2 + a_2K_2^2 + a_3K_2^3 = \varepsilon. \qquad (8)$$

Therefore, the unknown coefficients, a_0, a_1, a_2 and a_3, are defined as:

$$\Rightarrow \begin{cases} a_0 = -\varepsilon \\ a_1 = \frac{\varepsilon K_1^3 + (\varepsilon - 1)(2K_2^3 - 3K_1K_2^2)}{K_1^4K_2 - 2K_1^2K_2^2 + K_1K_2^3} \\ a_2 = \frac{-2\varepsilon K_1^3 + (\varepsilon - 1)(3K_1^2K_2 - K_2^3)}{K_1^4K_2 - 2K_1^3K_2^2 + K_1^2K_2^3} \\ a_3 = \frac{\varepsilon K_1^3 - (\varepsilon - 1)(2K_1^2K_2 - K_1K_2^2)}{K_1^5K_2 - 2K_1^4K_2^2 + K_1^3K_2^3} \end{cases} \qquad (9)$$

To involve the effect of upstream structure dimensions on scour similarity, the nondimensional coefficients, K_1 and K_2 could be determined by plotting the experimental values of $\frac{x_m}{w}$ and $\frac{x_s}{w}$ against the corresponding values of $\frac{y_m}{w}$, respectively. Figures 5 and 6 depict the values of K_1 and K_2 at different adverse slopes. However, to derive a general scour profile for all slopes, the average values of these parameters are shown in Figure 7. Variations of K_1 and K_2, with the slope of stilling basin (S_o), can be given as (Figure 8):

$$K_1 = -12.51S_o^2 - 6.189S_o + 2.745, \qquad (10)$$

$$K_2 = 2.107a\tan(-44.61S_o) + 6.95. \qquad (11)$$

It seems that the length of the scour hole and the horizontal distance of maximum scour depth increase with the slope of the stilling basin. Table 3 depicts the obtained coefficients, a_0, a_1, a_2 and a_3, related to the slope of the stilling basin. Also, a general scour profile for all slopes of the stilling basin and the proposed values by Dey and Sarkar [8] for scour profiles at the downstream of the horizontal rigid apron are presented in Table 3. Table 4 depicts the comparison of experimental and computed values of temporal scour depths from different nondimensional profiles. The results indicate the higher applicability of the proposed scour profiles for any slope of the stilling basin. Consequently, temporal scour profiles at the downstream of any bed slope are similar in shape.

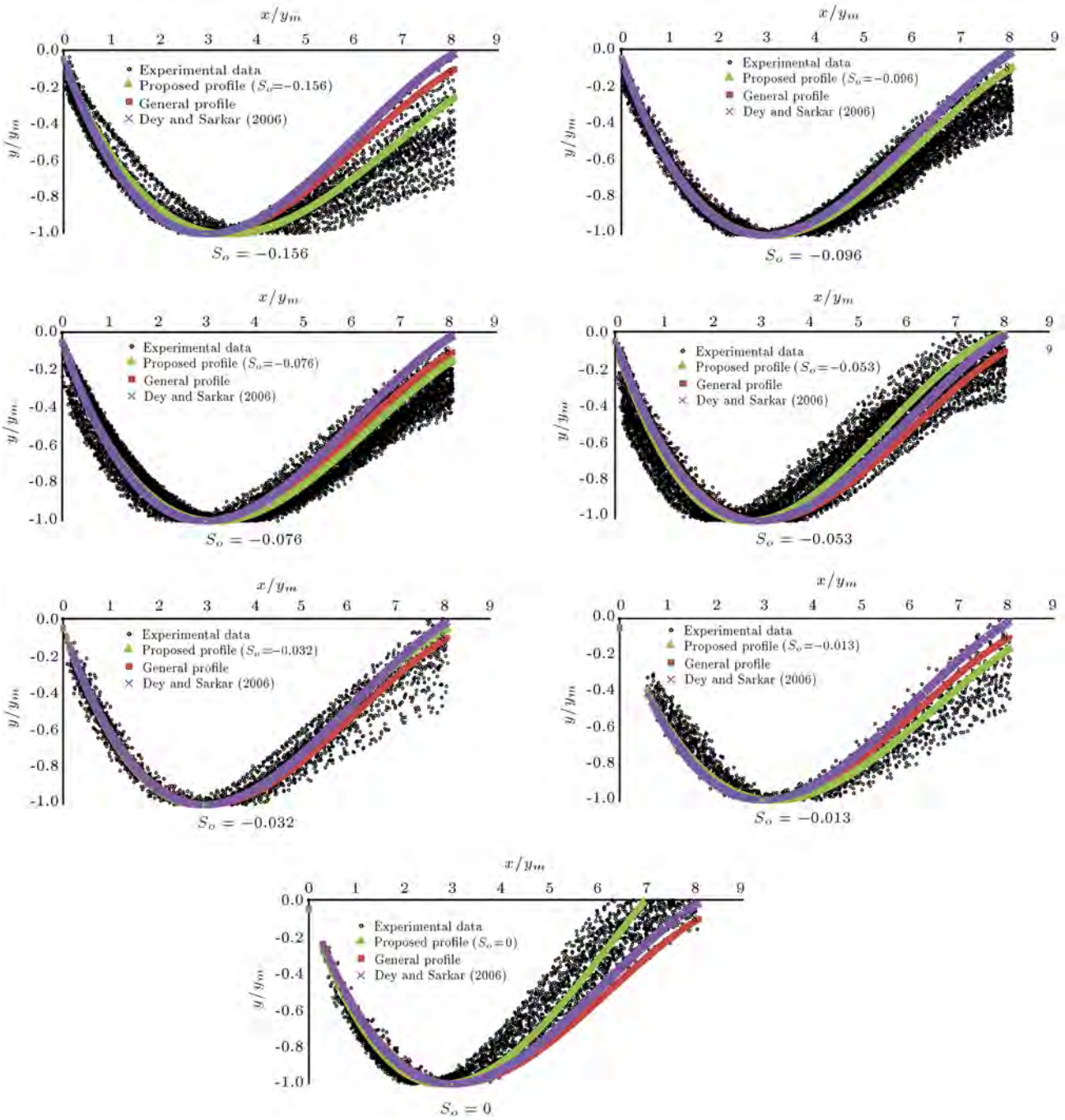

Figure 4. Nondimensional scour profiles at the downstream of different slopes of stilling basin.

However, the longitude evolution of the scour profile increased as the slope of the stilling basin increased, and its vertical dimension decreased.

Integrating from the temporal scour profiles (Eq. (4)) will give the total volume of scour per unit width of mobile bed at any time ($V_s(t)$):

$$V_s(t) = \int_{x=0}^{x=x_s} ydx = y_m^2 \int_{x=0}^{x=x_s} \left(\frac{y}{y_m}\right) d\left(\frac{x}{y_m}\right) = y_m^2 \left(a_0 K_2 + \frac{a_1}{2} K_2^2 + \frac{a_2}{3} K_2^3 + \frac{a_3}{4} K_2^4\right). \quad (12)$$

Figure 9 shows the volume of scour at any time against the slope of the stilling basin. It can be seen that the volume of the scour bed increases at the downstream of the adverse stilling basin in comparison to the horizontal one, due to its severe longitudinal development. Figure 9 yields:

$$\frac{V_s(t)}{y_m^2} = 6.056 - 1.536e^{12.42S_o}. \quad (13)$$

It is noteworthy to mention that the dune formation in the present study was overlooked. The sedimentation

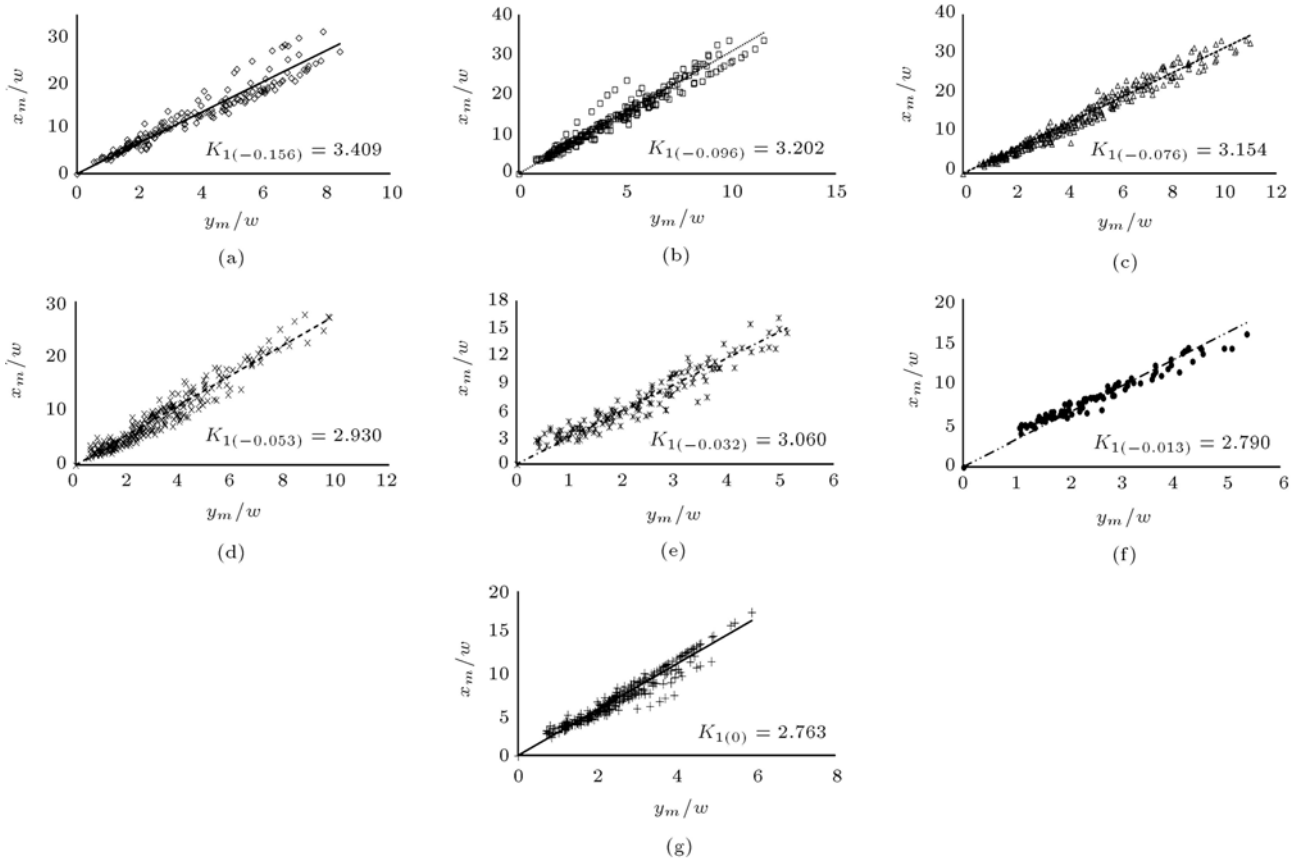

Figure 5. Determination of K_1 at different slopes of stilling basin.

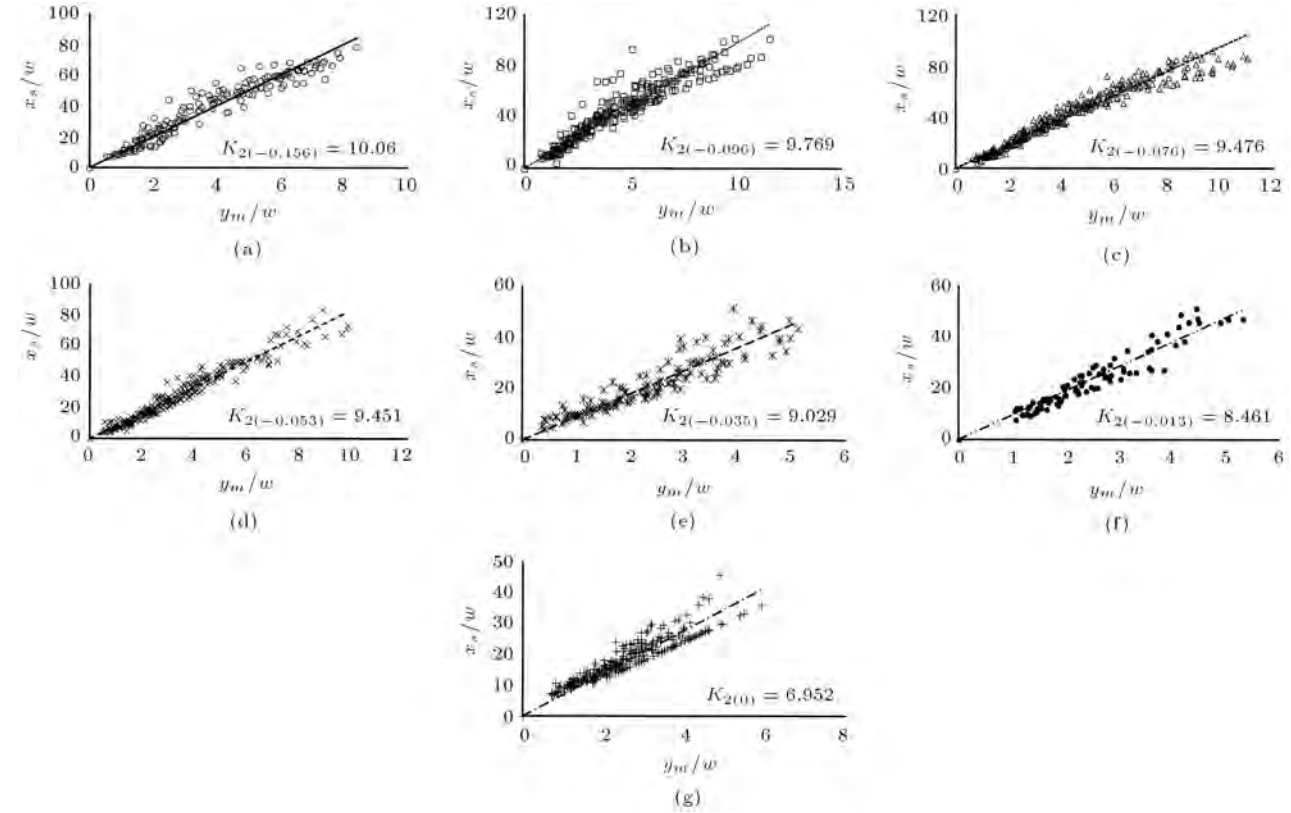

Figure 6. Determination of K_2 at different slopes of stilling basin.

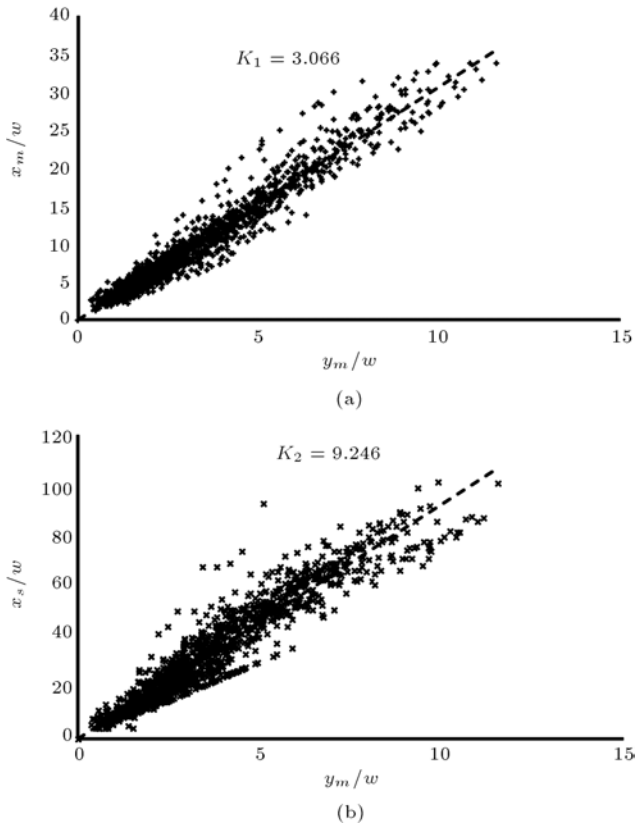

Figure 7. Average values of K_1 and K_2 to derive a general scour profile for all slopes of stilling basin.

Table 3. Coefficients of different equations for nondimensional scour profiles.

S_o	a_0	a_1	a_2	a_3
-0.156	-0.05	-0.6257	0.1218	-0.0059
-0.096	-0.05	-0.6969	0.1511	-0.0081
-0.076	-0.05	-0.6764	0.1424	-0.0074
-0.053	-0.05	-0.7722	0.1856	-0.0111
-0.032	-0.05	-0.7281	0.1651	-0.0093
-0.013	-0.05	-0.6661	0.1381	-0.0071
0	-0.05	-0.753	0.1737	-0.0093
General scour profile	-0.05	-0.6958	0.1507	-0.0081
Dey and Sarkar [8]	-0.05	-0.7169	0.1595	-0.0087

Table 4. Comparison of different scour profiles with the experimental data.

Type of scour hole	SE	R^2
Dey and Sarkar [8]	0.123	0.881
General scour profile	0.110	0.906
Proposed scour profiles for any bed slope	0.085	0.943

process in the prototype can occur differently in the model, unlike erosion. Consequently, this temporal phenomenon may not occur in field applications, although the scour hole characteristics are certainly affected by the dune.

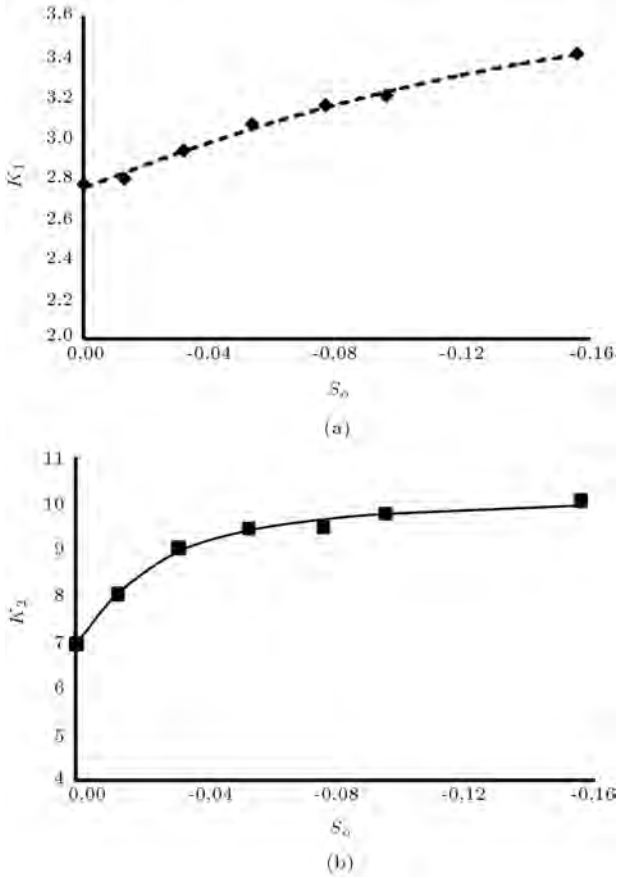

Figure 8. Variation of K_1 and K_2 with S_o.

3.4. Scour hole dimensions

A multiple regression analysis, based on experimental data, according to Eq. (3), yields the following relations to estimate the temporal dimensions of the scour hole:

$$\begin{cases} \frac{x_m}{w} = 4.51(1+\tan\theta)^{0.503}\left(\frac{y_t}{w}\right)^{-0.752}\left(\frac{L}{w}\right)^{-1.161} \\ \qquad (\mathrm{Fr}_1)^{1.46079}\left(\frac{t}{t_0}\right)^{0.271}\left(\frac{D_{50}}{w}\right)^{-0.475} \\ \frac{y_m}{w} = 0.486(1+\tan\theta)^{-0.342}\left(\frac{y_t}{w}\right)^{-0.635}\left(\frac{L}{w}\right)^{-1.006} \\ \qquad (\mathrm{Fr}_1)^{1.528}\left(\frac{t}{t_0}\right)^{0.271}\left(\frac{D_{50}}{w}\right)^{-0.538} \\ \frac{x_s}{w} = 0.281(1+\tan\theta)^{0.464}\left(\frac{y_t}{w}\right)^{-0.638}\left(\frac{L}{w}\right)^{-0.279} \\ \qquad (\mathrm{Fr}_1)^{1.549}\left(\frac{t}{t_0}\right)^{0.255}\left(\frac{D_{50}}{w}\right)^{-0.403} \end{cases} \quad (14)$$

To present scour characteristics at the quasi equilibrium stage, experimental data after 24 hr were used. It is assumed that the scour hole reaches an equilibrium stage in this time. This is a conservative assumption, especially for longitudinal development. The scour hole reaches an equilibrium stage in the depth direction, while the scour process continues due to fine grain movement along the hole. In this state, the maximum depth of the scour hole is approximately constant, while the scour profile will

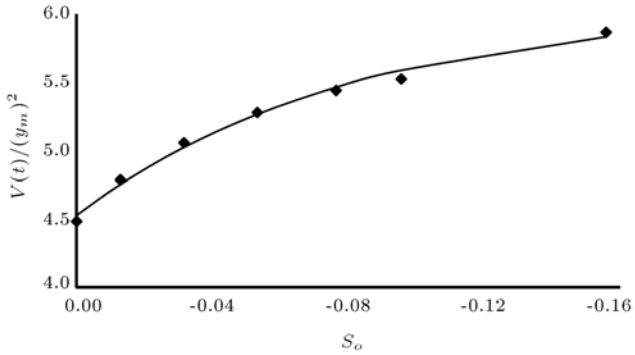

Figure 9. Variation of $V_s(t)$ with S_o.

change. Moreover, the equilibrium time depends on the sediment size and flow conditions. Considering the above mentioned, the following relations are suggested to estimate the scour hole dimensions at the semi-equilibrium phase:

$$\begin{cases} \frac{x_{me}}{w} = 91.562(1+\tan\theta)^{0.124}\left(\frac{y_t}{w}\right)^{-1.029}\left(\frac{L}{w}\right)^{-0.944} \\ \qquad (\mathrm{Fr}_1)^{1.52}\left(\frac{D_{50}}{w}\right)^{-0.327} \\ \frac{y_{me}}{w} = 13.018(1+\tan\theta)^{-0.614}\left(\frac{y_t}{w}\right)^{-0.888}\left(\frac{L}{w}\right)^{-0.753} \\ \qquad (\mathrm{Fr}_1)^{1.403}\left(\frac{D_{50}}{w}\right)^{-0.367} \\ \frac{x_{se}}{w} = 29.069(1+\tan\theta)^{0.679}\left(\frac{y_t}{w}\right)^{-0.881}\left(\frac{L}{w}\right)^{-0.452} \\ \qquad (\mathrm{Fr}_1)^{1.466}\left(\frac{D_{50}}{w}\right)^{-0.291} \end{cases} \quad (15)$$

The range of applicability of the above regression relations is $0 \le \tan\theta \le 0.156{,}1.74 \le \frac{y_t}{w} \le 15.19{,}3.78 \le \mathrm{Fr}_1 \le 11.14{,}25.1 \le \frac{L}{w} \le 84.3{,}0.041 \le \frac{D_{50}}{w} \le 0.127$. Using the experimental data, $\frac{y_m}{w}$ and $\frac{y_{me}}{w}$ are computed from Eqs. (14) and (15), respectively, and compared with the observed data in Figure 10. The regression coefficient (R^2), and standard error (SE), between the observed and computed results, indicate that Eqs. (14) and (15) correspond satisfactorily with the experimental data. The above regression relations generally depict the effects of different parameters on the geometric dimensions of the scour hole (x_{me}, y_{me}, x_{se}). It is evident that the scour dimensions increase by an increase in the approaching Froude number. The maximum scour depth increases as the grain size is reduced. Clearly, this result is simply a reflection of the increased resistance to an imposed shear stress of larger sized particles. Accordingly, the location of the point of maximum scour depth moves downstream, as with a decrease in the grain size, and the length of the scour hole was increased. It can be seen that the maximum depth of the scour hole decreases by increasing the length and slope of the stilling basin, while the longitudinal dimensions of the hole increase. Flow lines at the end of the adverse stilling basins tended towards the water surface and impinged on the scour bed with less shear stress. The hydrodynamic bed shear stress decreased as the length and slope of

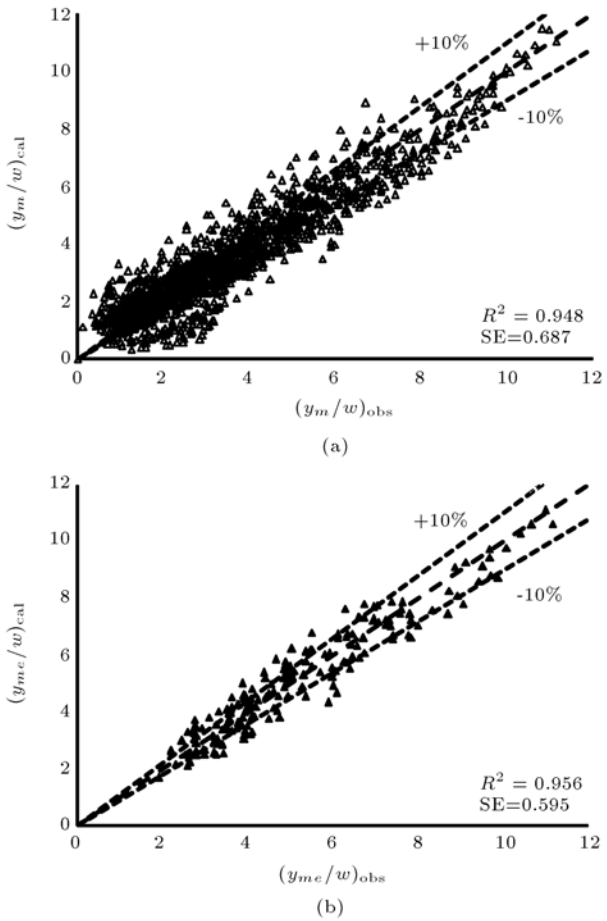

Figure 10. Comparison of the scour depths (y_m, y_{me}) at the downstream of all slopes computed using Eqs. (14) and (15) with the experimental data.

the stilling basin increased, and the impingement point moved downstream. Consequently, the scour profile at the downstream of the adverse stilling basins was severely developed in longitudinal dimensions, whereas its depth was decreased. Considering Eq. (14) reveals that the maximum scour depth and its location change with an equivalent time rate, while the length of the hole requires more time to reach an equilibrium phase. This is probably due to a higher requirement of shear stress to overcome the weight of the grains on the sloping bed. An interesting problem is the effect of tailwater depth on maximum local scour depth at the downstream of adverse stilling basins. it can be observed from Eq. (15) that the equilibrium scour depth increases as the tailwater depth is reduced. This is in contradiction with the reported regression relation by Dey and Sarkar [8], which resulted in a general increase in equilibrium scour depth with tailwater depth at the downstream of horizontal rigid aprons. It is noteworthy to mention that the tailwater depth reduces in the presence of an adverse stilling basin. Moreover, the hydraulic jump on adverse basins is an unstable phenomenon, which

requires manual control of tailwater depth to keep in the basin. This instability can be controlled by increasing retrograde forces (pressure force at the end of the basin and the weight of water volume) rather than repelled force (pressure force at the approaching section). At low tailwater depths, the hydraulic jump was repelled out of the stilling basin, due to overcoming the repelled force, and resulted in severe erosion in the sand bed. As the tailwater depth increases, the retrograde forces overcome the hydrodynamics force and the hydraulic jump is returned to the rigid apron. Consequently, the hydrodynamic bed shear stress on the hole is reduced, and after a critical tailwater depth, the maximum scour depth decreases to reach a constant value. Figure 11(a) shows the dependence of the normalized scour depth ($\frac{y_{mc}}{w}$) on relative tailwater depth ($\frac{y_t}{w}$) at the downstream of adverse stilling basins. It can be seen that a critical tailwater depth prevails when the scour depth reaches a maximum value. Using experimental data in the presence of horizontal rigid aprons, the following relations are proposed to estimate the scour hole dimensions. For temporal evaluation, the scour hole dimensions could be determined by using the following equations:

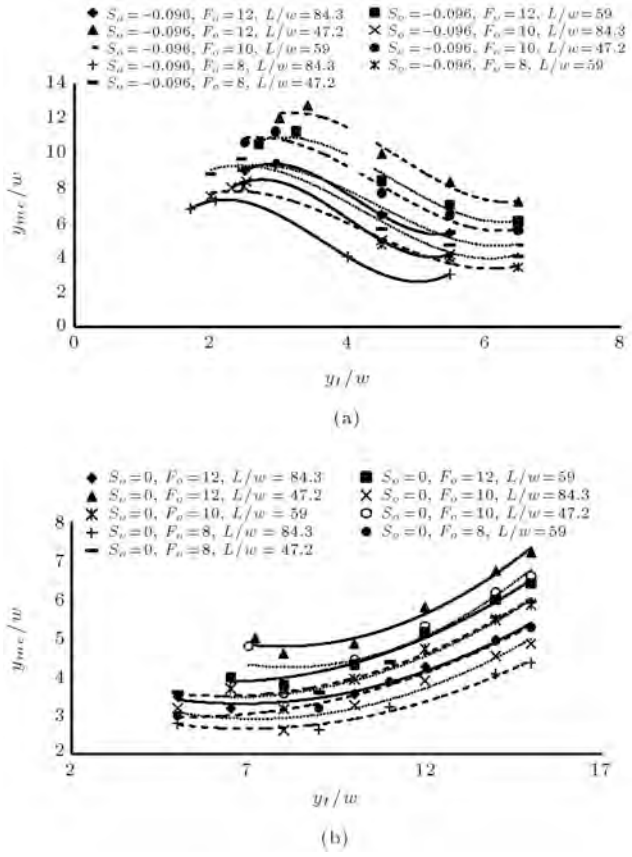

Figure 11. The effect of tailwater depth on maximum equilibrium scour depth at the downstream of a) adverse stilling basin, and b) horizontal stilling basin.

$$\begin{cases} \frac{x_m}{w} = 0.177\left(\frac{y_t}{w}\right)^{0.956}\left(\frac{L}{w}\right)^{-0.818} \\ \qquad (\mathrm{Fr}_1)^{0.937}\left(\frac{t}{t_0}\right)^{0.214}\left(\frac{D_{50}}{w}\right)^{-0.321} \\ \frac{y_m}{w} = 0.027\left(\frac{y_t}{w}\right)^{0.968}\left(\frac{L}{w}\right)^{-0.717} \\ \qquad (\mathrm{Fr}_1)^{0.983}\left(\frac{t}{t_0}\right)^{0.237}\left(\frac{D_{50}}{w}\right)^{-0.362} \\ \frac{x_s}{w} = 0.131\left(\frac{y_t}{w}\right)^{0.852}\left(\frac{L}{w}\right)^{-0.468} \\ \qquad (\mathrm{Fr}_1)^{0.909}\left(\frac{t}{t_0}\right)^{0.216}\left(\frac{D_{50}}{w}\right)^{-0.358} \end{cases} \tag{16}$$

and at equilibrium phase,

$$\begin{cases} \frac{x_{mc}}{w} = 3.059\left(\frac{y_t}{w}\right)^{0.503}\left(\frac{L}{w}\right)^{-0.643} \\ \qquad (\mathrm{Fr}_1)^{0.999}\left(\frac{D_{50}}{w}\right)^{-0.228} \\ \frac{y_{mc}}{w} = 0.732\left(\frac{y_t}{w}\right)^{0.98}\left(\frac{L}{w}\right)^{-0.532} \\ \qquad (\mathrm{Fr}_1)^{0.482}\left(\frac{D_{50}}{w}\right)^{-0.245} \\ \frac{x_{sc}}{w} = 3.923\left(\frac{y_t}{w}\right)^{0.318}\left(\frac{L}{w}\right)^{-0.364} \\ \qquad (\mathrm{Fr}_1)^{0.942}\left(\frac{D_{50}}{w}\right)^{-0.249} \end{cases} \tag{17}$$

It can be seen from Eqs. (16) and (17) that the scour depth generally increases with tailwater depth, which is in agreement with previous studies [8]. Figure 11(b) depicts the effect of tailwater depth on the maximum equilibrium scour depth at the downstream of horizontal rigid aprons. It is shown that the scour depth initially decreases with an increase in tailwater depth, and, after a certain tailwater depth, tends to increase. This trend was also reported by Ali and Lim [18] and Dey and Sarkar [8]. The corresponding magnitudes of regression correction and standard error in Figure 12 shows reasonable agreement between the two sets of data from experiments and Eqs. (16) and (17).

3.5. Three dimensional of the scour hole

Figure 13 shows the 3D development of the scour hole. It can be seen that the maximum depth of the scour hole at any distance from the basin occurs in the vicinity of the channel side walls and decreases to the centerline. Consequently, the above mentioned scour profiles give the maximum erosion of the scour hole for a conservative design. Moreover, the local scour process at the downstream of a submerged sluice gate is a three dimensional phenomenon, and channel width affects the hole dimensions. This is probably due to random velocities at the downstream of the hydraulic jump. A set of flow lines tend to channel side walls and cause severe erosion in these areas. Eroded sediment is piled up at the centerline and decreases the scour depth in this section. However, it is expected that there is a minimum value for the ratio of channel width to gate opening whose scour profiles are independent of scale effects.

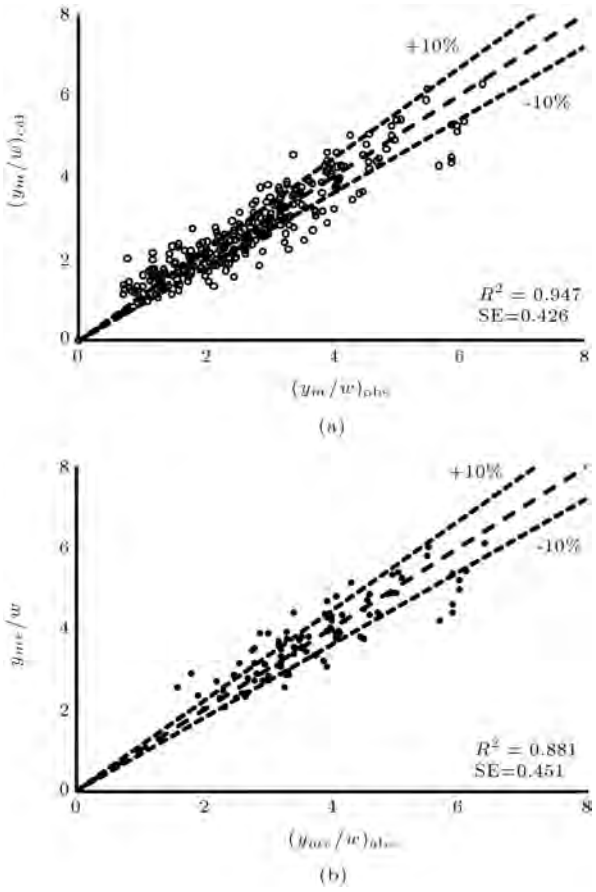

Figure 12. Comparison of the scour depths (y_m, y_{me}) at the downstream of horizontal stilling basin computed using Eqs. (16) and (17) with the experimental data.

3.6. Time variation of maximum scour depth

Figure 14 shows the typical time variation of maximum scour depth (y_m), the distance of maximum scour depth from the end of the rigid apron (x_m), the length of scour hole (x_s), and scour volume per unit width (V_s) after 54 hr testing. It is shown that:

$$\frac{x_{m(t=24\text{hr})}}{x_{m(t=54\text{hr})}} = 0.863, \quad \frac{y_{m(t=24\text{hr})}}{y_{m(t=54\text{hr})}} = 0.875,$$

$$\frac{x_{s(t=24\text{hr})}}{x_{s(t=54\text{hr})}} = 0.846, \quad \frac{V_{s(t=24\text{hr})}}{V_{s(t=54\text{hr})}} = 0.79.$$

Moreover, Balachandar and Kells [19] reported that the maximum depth scour and the nondimensional volume of scour followed a power-law relationship with time, with equilibrium not yet achieved by the end of the 144 hr test.

Farhoudi and Smith [3] suggested a power-law equation for the time variation of scour depth related to the dimension of the structure, as:

$$\frac{y_m}{d_o} = k\left(\frac{t}{T}\right)^{\alpha}, \tag{18}$$

in which d_o is a characteristic depth, T is the time taken for the characteristic depth for scour, d_o, to be reached, and t is the time at which a maximum scour depth of y_m has been reached and coefficients k and α are to be determined. In the present study, an obvious choice for d_o was a dimension related to the linear dimensions of the sluice gate and a value of $d_o = 2w$ was considered.

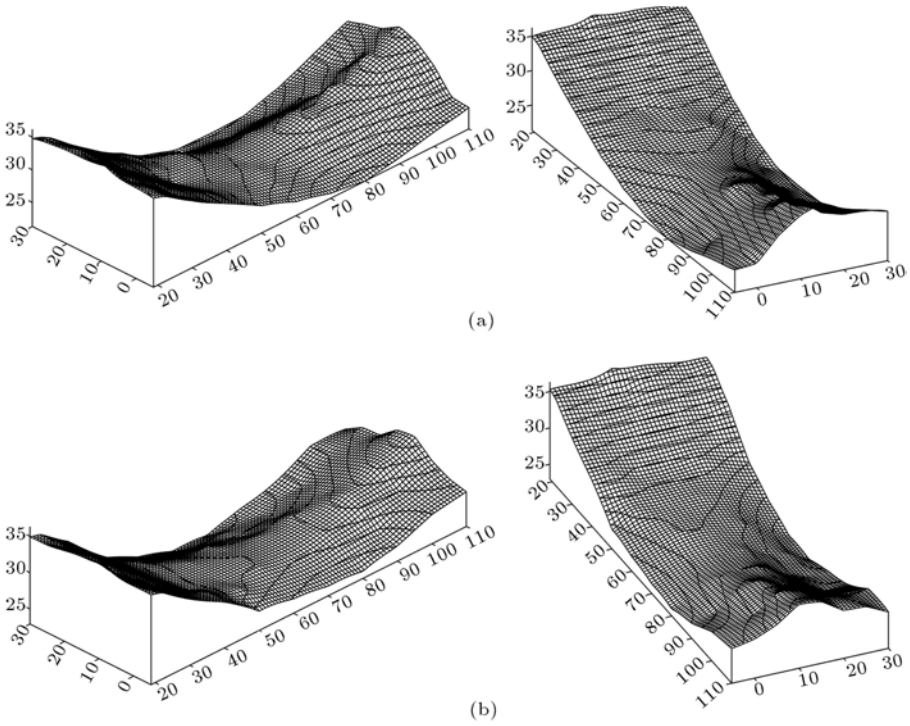

Figure 13. 3D development of scour hole: a) $S_o = -0.0156$, $D_{50} = 1.11$ mm; and b) $S_o = -0.076$, $D_{50} = 0.58$ mm.

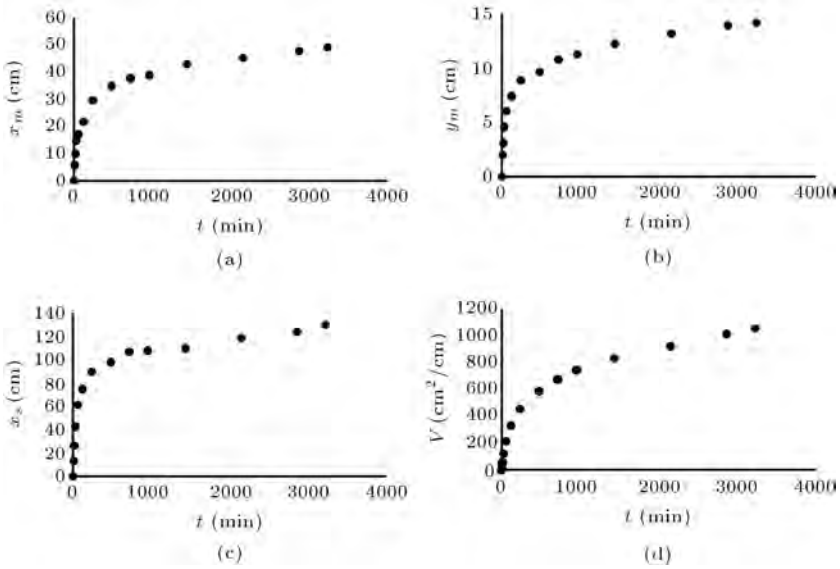

Figure 14. Time variation of scour hole dimensions for 56 hr test.

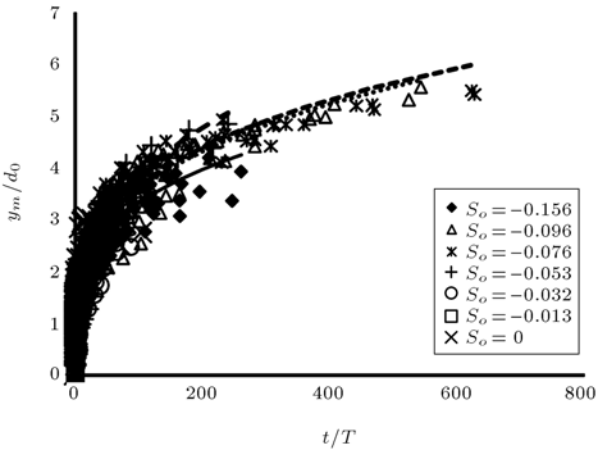

Figure 15. Determination of k and α at different slopes of stilling basin.

The time required to reach a scour depth equal to $2w$ could be estimated by using the following equation:

$$T = 10.345(1+\tan\theta)^{1.357}\left(\frac{L}{w}\right)^{3.556}\left(\frac{D_{50}}{w}\right)^{1.481}\left(\frac{y_t}{w}\right)^{3.346}(\mathrm{Fr}_1)^{-5.628}. \quad (19)$$

Figure 15 depicts the variation of the maximum temporal scour depths at the downstream of adverse stilling basins, where the coordinates were normalized. This figure gives the coefficients of k and α related to the slope of the stilling basin. It is shown that the coefficients of k and α decrease by increasing S_o. Consequently, more time is required to reach a certain value of scour depth at the downstream of the adverse stilling basin in comparison with the horizontal one. k and α can be given as functions of S_o (Figure 16):

$$\begin{cases} k = -15.856S_o^2 - 0.452S_o + 0.986 \\ \alpha = \frac{1}{3.08 - 12.86S_o - 46.26S_o^2} \end{cases} \quad (20)$$

Table 5. Comparison of k and α at the downstream of hydraulic structures.

Type of hydraulic structure	Researcher	α	k
Estuary closure structure without any hydraulic jump	Breusers [2]	0.38	1
Spillway	Frahoudi and Smith [3]	0.19	1
Spillway with positive-step stilling basin	Oliveto et al. [10]	0.2	0.92
Sluice gate with horizontal rigid apron	Present study	0.32	0.986

Table 5 compares the coefficients in the power-law equation, which developed at the downstream of different hydraulic structures. The results imply that the values of k and α and maximum scour depth at the downstream of the sluice gates are greater than the spillways.

4. Conclusion

This experimental study of scouring, downstream of a submerged sluice gate with an adverse stilling basin, led to the following conclusions.

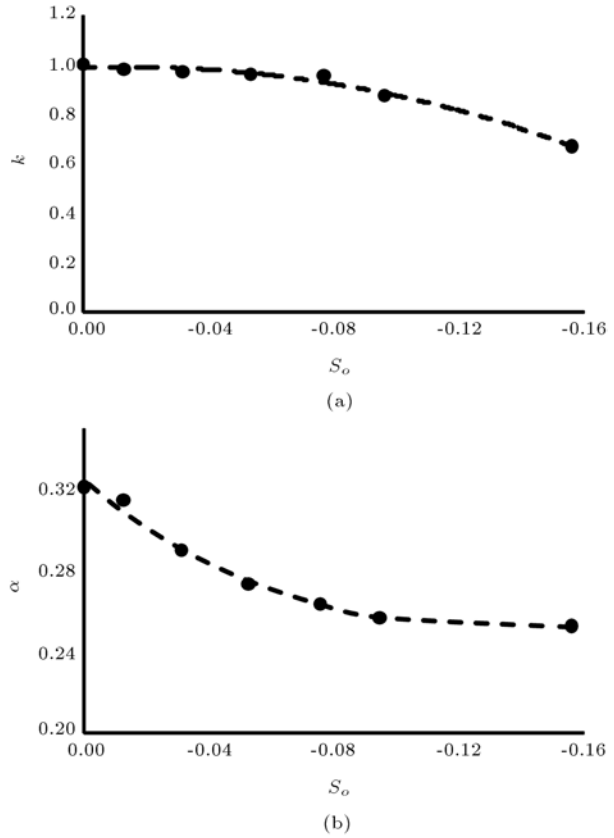

Figure 16. Variation of k and α with S_o.

1. The temporal scour profiles at the downstream of any bed slope are similar in shape and have been expressed by a polynomial equation;
2. The longitude evolution of the scour profile increased as the slope of the stilling basin increased;
3. The volume of the scour bed increases at the downstream of the adverse stilling basin in comparison with the horizontal one, due to its severe longitudinal development;
4. The maximum depth of the scour hole at any distance from the basin occurs in the vicinity of the channel side walls and decreases to the centerline;
5. Some regression relations were obtained based on experimental data to estimate temporal scour hole dimensions to reach an equilibrium stage;
6. It was observed that the maximum depth of the scour hole decreased, as the length and slope of the stilling basin increased, while the longitudinal dimensions of the hole increased;
7. Under specific conditions at the downstream of adverse stilling basins, the depth of the scour hole reaches a maximum value and then decreases to reach a constant value as the tailwater depth increases;
8. Scour depth at the downstream of horizontal rigid aprons initially decreases with increasing tailwater depth, and, after a certain tailwater depth, the depth of the scour hole tends to increase;
9. The time variation of scour depth has been scaled by a power-law equation. The coefficients of this equation decrease with an increase in the slope of the stilling basin.

Nomenclature

a_{0-3}	Coefficients;
C_u	Uniformly coefficient;
d_o	A dimension related to the linear dimensions of the sluice gate ($d_o = 2w$);
D_{10}	10% finer sediment size;
$D_{15.9}$	15.9% finer sediment sizes;
D_{50}	Median sediment size;
D_{60}	60% finer sediment size;
$D_{84.1}$	84.1% finer sediment size;
D_{90}	90% finer sediment size;
Fr_1	Approaching Froude number;
F_o	Densimetric Froude number ($F_o = \frac{q}{\sqrt{g(s_s-1)D_{50}^3}}$);
g	Acceleration due to the gravity;
k	Factor in scour development relationship;
L	Length of stilling basin;
q	Flow discharge per unit width of the rectangular basin;
S_o	Slope of stilling basin;
t	Time from beginning of scour development;
T	Time taken for the maximum scour depth to equal;
$V_s(t)$	Volume of scour hole per unit width at time;
w	Gate opening;
x	Horizontal distance;
x_m	Horizontal distance of maximum scour depth from the stilling basin at time;
x_{me}	Horizontal distance of maximum equilibrium scour depth from the stilling basin;
x_s	Length of scour hole at time;
x_{se}	Length of scour hole at equilibrium stage;
y	Vertical distance;
y_1	Flow depth at the vena contracta;
y_{me}	Maximum equilibrium local scour depth;

y_m	Maximum scour depth at time;
y_t	Tailwater depth;
α	Exponent in scour development relationship;
ε	Factor;
ϕ	Angle of repose;
v	Fluid kinematic viscosity;
γ	Specific weight of water;
θ	Angle of bed slope;
ρ	Mass density of fluid;
ρ_s	Mass density of sediment;
σ_g	Geometric standard deviation.

References

1. Laursen, E.M. "Observations on the nature of scour", *Proceedings of the 5th Hydraulic Conference*, Bulletin 34, State University of Iowa, Iowa, USA, pp. 179-197 (1952).
2. Breusers, H.N.C. "Conformity and time scale in two-dimensional local scour", *Proceedings of the Symposium on Model and Prototype Conformity*, Hydraulics research laboratory, Poona, India, pp. 1-8 (1966).
3. Farhoudi, J. and Smith, K.V.H. "Time scale for scour downstream of hydraulic jump", *Journal of the Hydraulics Division*, **108**(10), pp. 1147-1162 (1982).
4. Hassan, N.M.K.N. and Narayanan, R. "Local scour downstream of an apron", *Journal of Hydraulic Engineering*, **111**(11), pp. 1371-1385 (1985).
5. Farhoudi, J. and Smith, K.V.H. "Local scour profiles downstream of hydraulic jump", *Journal of Hydraulic Research*, **23**(4), pp. 342-358 (1985).
6. Chatterjee, S.S., Ghosh, S.N. and Chatterjee, M. "Local scour due to submerged horizontal jet", *Journal of Hydraulic Engineering*, **120**(8), pp. 973-992 (1994).
7. Dargahi, B. "Scour development downstream of a spillway", *Journal of Hydraulic Research*, **41**(4), pp. 417-426 (2003).
8. Dey, S. and Sarkar, A. "Scour downstream of an apron due to submerged horizontal jets", *Journal of Hydraulic Engineering*, **132**(3), pp. 246-257 (2006).
9. Dey, S. and Sarkar, A. "Effect of upward seepage on scour and flow downstream of an apron due to submerged jets", *Journal of Hydraulic Engineering*, **133**(1), pp. 59-69 (2007).
10. Oliveto, G., Comuniello, V. and Bulbule, T. "Time-dependent local scour downstream of positive step stilling basins", *Journal of Hydraulic Research*, **49**(1), pp. 105-112 (2011).
11. Ghodsian, M., Mehraein, M. and Ranjbar, H.R. "Local scour due to free fall jets in non-uniform sediment", *Scientia Iranica, Transactions A: Civil Engineering*, **19**(6), pp. 1437-1444 (2012).
12. McCorquodale, J.A. and Mohamed, M.S. "Hydraulic jumps on adverse slopes", *Journal of Hydraulic Research*, **32**(1), pp. 119-130 (1994).
13. Pagliara, S. and Peruginelli, A. "Limiting and sill-controlled adverse-slope hydraulic jump", *Journal of Hydraulic Engineering*, **126**(11), pp. 847-851 (2000).
14. Rajaratnam, N. "The hydraulic jump in sloping channels", *Journal of Irrigation and Power*, **23**(2), pp. 137-149 (1966).
15. Baines, P.G. and Whitehead, J.A. "On multiple states in single-layer flows", *Physics of Fluids*, **15**(2), pp. 298-307 (2003).
16. Breusers, H.N.C. and Raudkivi, A.J. "Scouring", *Hydraulic Structure Design Manual*, A.A. Balkema, Rotterdam, The Netherlands (1991).
17. Lambe, T.W. and Whitman, R.V., *Soil Mechanics*, SI Version, John Wiley, New York, USA (1969).
18. Ali, K.H.M. and Lim, S.Y. "Local scour caused by submerged wall jets", *Proceedings Institution of Civil Engineers*, London, England, **81**(2), pp. 607-645 (1986).
19. Balachandar, R. and Kells, J.A. "Local channel scour in uniformly graded sediments: The time-scale problem", *Canadian Journal of Civil Engineering*, **24**(5), pp. 799-807 (1997).

Biographies

Hossein Khalili Shayan received a BS degree in Water Engineering, in 2009, from Urmia University, Iran, and an MS degree, in 2012, from the University of Tehran, Iran. His research interests include open channel hydraulics, investigation of hydraulic behavior of irrigation structures, local scour at the downstream of hydraulic structures and seepage phenomena under diversion dams.

Javad Farhoudi received his PhD degree in Hydraulic Structures from Southampton University, UK, in 1979, and is currently Distinguished Professor of Hydraulic Structures and River Engineering in the Department of Irrigation and Reclamation Engineering, Faculty of Agricultural Engineering and Technology (UTCAN) at the University of Tehran, Iran. He has served higher education in the field of Irrigation and Hydraulic Engineering since 1974, and worked on the design of hydraulic structures in Iran. Dr. Farhoudi has also served on several committees and commissions in the field of water resources engineering, such as ICOLD, ICID, IHP and the Iranian Academy of Sciences, and has published numerous papers in refereed national and international journals and conferences in these areas of expertise.

His research interests include scouring and pressure fluctuation encountered in stilling basins, as well as flow measuring structures.